Northumbria Research Link

Citation: Qureshi, Yumna, Tarfaoui, Mostapha, Lafdi, Khalil K. and Lafdi, Khalid (2020) In-Situ Monitoring, Identification and Quantification of Strain Deformation in Composites Under Cyclic Flexural Loading Using Nylon/Ag Fiber Sensor. IEEE Sensors Journal, 20 (10). pp. 5492-5500. ISSN 1530-437X

Published by: IEEE

URL: https://doi.org/10.1109/jsen.2020.2969329 <https://doi.org/10.1109/jsen.2020.2969329>

Northumbria University
NEWCASTLE

In-situ Monitoring, Identification and Quantification of Strain Deformation in Composites under Cyclic Flexural Loading using Nylon/Ag Fiber Sensor

Yumna Qureshi, Mostapha Tarfaoui, Khalil K. Lafdi, and Khalid Lafdi
mailto:mostapha.tarfaoui@ensta-bretagne.frmailto:ing@gmail.commailto:klafdi1@udayton.edu

***Abstract*— Despite having vast structural applications, Composites are not exempt from limitations and are susceptible to deforming during operation. Therefore, it is essential to develop in-situ monitoring systems to avoid their catastrophic failure or high repairing cost. So, the objective of this study was to monitor the deformation behavior of composites subjected to cyclic flexural deformation in real-time using a Nylon/Ag fiber sensor. Nylon/Ag fiber sensor was integrated at different direction i.e. 0°, +45°, 90°, -45° gradually between each ply of the composite specimens which were then machined in star shape where each leg signified the direction of the sensor. These specimens were then tested under cyclic flexural deflection at the strain rate of 2mm/min for 10 cycles. Mechanical results of composite specimens and electrical response of each Nylon/Ag sensor fiber showed excellent repeatability however, each Nylon/Ag fiber sensor showed a specific resistance behavior because of their respective position. The increase or decrease in the resistance of the fiber sensor signified the presence of tensile or compressive strain respectively and the intensity of the signal quantified the amount of deformation. The results confirmed that the fiber sensor showed good potential as flexible sensor reinforcement in composites for in-situ monitoring, identification and quantification of the deformation.**

***Index Terms*— Composite structures; Mechanical Deformations; In-situ strain monitoring; fiber sensor.**

I. Introduction

Composites have substituted traditional materials in almost every engineering and structural applications because of their extraordinary mechanical strength, low density, structural durability, resistance to environmental factors and cost effectiveness however, even they have limitations and are prone to damage such as fiber cracking, matrix failure, delamination, thermal deformation and environmental degradation [1ï 4]. So, it is essential to monitor their behavior during extreme loading situations or environmental surroundings to avoid their sudden failure [5ï 7]. Structural health monitoring (SHM) is a well-known technique widely use to monitor the performance of materials in working conditions to ensure safe and reliable structures [8].

Yumna Qureshi and Mostapha Tarfaoui are with IRDL (UMR CNRS 6027) / PTR-1/ PTR-1, ENSTA BRETAGNE, 2, rue François VERNY, 29806 BREST CEDEX 9, Bretagne, France, e-mail: yumna.qureshi@ensta-bretagne.org (Corresponding author: Y. Qureshi), e-mail: mostapha.tarfaoui@ensta-bretagne.fr (Corresponding author: M. Tarfaoui)

Khalil K. Lafdi and Khalid Lafdi are with Nanomaterials Laboratory, University of Dayton, Dayton, 45469-0168, Ohio, United States, e-mail: khalilboeing@gmail.com, e-mail: klafdi1@udayton.edu

Khalid Lafdi is with Department of Mechanical and Construction Engineering, Northumbria University, Newcastle upon Tyne, UK, email: khalid.lafdi@northumbria.ac.uk

These monitoring systems were established progressively over the time from non-destructive methods to in-situ monitoring of materials [9ï12]. Numerous studies had frequently designed systems to detect strain deformation and various types of failures such as thermal deformation, fiber cracking, debonding/delamination etc. in composites using different SHM methods under flexural deflection however, very less or no information was available about the influence of the location of the sensor on their sensitivity and damage detection [13ï19]. Furthermore, no evidence is available in the literature to understand the response of the sensor in differentiating and quantifying damage during flexural deformation.

The change in electrical resistance measurement (ER) in which resistance change of the material is measured during operation was one of the in-situ SHM technique used for monitoring the performance of composites during operation [21ï25]. It was often used for carbon fiber reinforced polymer composites (CFRP) because of their good electrical conductance and worked based on contact change and rearrangement of carbon fibers with in composites during deformation [26,27]. The response signal of resistance change in this technique was in direct correlation to the applied strain in case of unidirectional (UD) fiber composites but was more complexed for composites with randomly dispersed fibers specifically in applications with large deformation such as bending [28ï31]. Besides, this technique was considered unfavorable for cementitious composites or glass fiber reinforced polymer (GFRP) composites because of their high resistivity which required addition of nano fillers to improve their self-sensing performance [32,33]. However, increasing the conductivity of the composites structures with the addition of nano fillers was not applicable on large scaled structures because it would require huge percentage of nano fillers to achieve good conductance behavior that could also result in dispersion problems and high cost [32,33].

Flexible smart textiles were than considered to be a favorable alternative for the SHM of structural composites because after insertion, they could not only monitor the deformation of the structure but also act as reinforcement [34ï37]. This working principle of these flexible conductive sensors i.e. textiles, fabrics and yarns, is similar to that of traditional strain gauges [35].

Conductive polymers were first used for in-situ damage monitoring of composites however, their conductivity was less as compared to nano particles and they were unstable under environmental effects [38ï41]. Likewise, inserting or coating conductive nano particles for example graphene, carbon black, carbon nanotubes (CNTs), etc. on polymeric yarns and fabrics were also considered for in-situ SHM of structures [41].

CNTs based fibers were used numerous times for in-situ structural health monitoring of composites because of their outstanding impact resistance, flexibility and high sensitivity [43,44]. In addition to damage detection, these ultra-high sensitive sensors were also studied for wearable devices and electronic skins for medical applications [44,45]. However, the sensitivity of CNT based sensors could be affected after insertion into the composite structures for two reasons, first is the porous network of CNTs which is permeable to resin molecules and second is the tunneling effect [46ï49]. In addition, sensors developed with reduced graphene oxide (RGO) also showed good flexibility, sensitivity with good stability in in-situ monitoring of high strain applications and did not show any resin penetration because of their surface and geometry conformability [50]. RGO based conductive elastomer composites had been used in strain monitoring of rubber seal because of their high sensitivity with GF higher than 143 and high flexibility with strain sensing range up to 170 [51]. However, RGO is toxic in nature and had stability issues when exposed to air [53,54].

Furthermore, metal nanoparticles such as nickel, gold, aluminum, copper, silver and stainless steel were also used for in-situ SHM application but among all these nano particles, silver (Ag) had great potential as coating material on flexible substrates such as polymer textiles and yarns because of its stability in air, competitive price, good conductivity and mechanical performance [54ï57]. Silver nano wires (AgNWs) had been studied as capacitive touch sensor when deposited on polymeric composite structure and successfully demonstrated its application as sensing human touch even in folded state [58]. In additions, Ag nano particles had already been studied for anti-microbial activities and in medical monitoring as wearable electronic clothes with good responsivity, stability and repeatability in strain sensing signals [60ï62]. However, application of Ag coated fabric regarding SHM of composites is still limited. Y. Qureshi et al. [62,63] recently investigated the application of Ag coated nylon yarn as strain sensor under tensile loading and found that the position of Nylon/Ag sensor wire played an important part in identification of type of strain and damage [64]. Moreover, they also found out in their extended study that position of Nylon/Ag sensor wire, at different locations through thickness in respective specimens but in same direction, differentiated in type of strain and damage in each specimen subjected to flexural loading up to fracture [65]. However no or very little information is available regarding the use of flexible sensor wires [62] when placed in different directions i.e. 0°, +45°, 90°, -45° to detect strain deformation in composites subjected to flexural deformation and to study the combined complex deformation behavior of composites through plies and with in plies.

Accordingly, an experimental study was conducted to examine the in-situ monitoring capability of Nylon/Ag fiber sensor for the deformation of composite material during repeated flexural loading. The fiber sensors were placed in different directions i.e. 0°, +45°, 90°, -45° regarding the roller axis and each fiber sensor in individual positions was separated by the single ply in all three specimens. The results presented interesting behaviors and indicated that the fiber sensor did not only monitored the deformation in each cycle but also demonstrated that the location and direction of the sensor played an important part in differentiating and quantifying different types of deformations.

II. Experimental Setup

A. Fabrication Procedure

Nylon/Ag fiber sensors were developed by depositing Ag nanoparticles as uniform continuous film on every filament of Nylon by using electroless plating process because of its effectiveness and simplicity in use even for complex substrates/geometries. The complete process is described in detail in [63] and has been presented in Figure 1. Briefly described, in this process, nylon yarn was cleaned with ethanol to remove any surface impurities then treated with silver nitrate ($AgNO_3$) and sodium hydroxide (NaOH) at 130°C for 2 hours. After that, reduction process in ammonia (NH_3) environment was carried out for a period of 2 hours which reduced the Ag(I) to Ag(0) ions and finally, silver nanoparticles were deposited on the surface of nylon. Scanning electron microscopy (SEM) further verified the homogeneous deposition of Ag nanoparticles on every filament of the Nylon yarn [64], Figure 2. Then the fiber sensor was cut into specific length and was inserted between the plies of chopped glass fibers in their respective position and direction during the fabrication of the composite specimen. Five plies of chopped glass fiber were used for reinforcement and to separate the fiber sensor from each other. In addition, the chopped fiber mat ensured isotropic mechanical behavior with poor conductivity and electrical isolation for each fiber sensor. Nylon/Ag fiber sensors were inserted in the specimen in their particular direction such that sensor A was in 0° between plies 1 and 2, sensor B was in 45° between plies 2 and 3, sensor C was in 90° between plies 3 and 4 and sensor D was in -45° between plies 4 and 5 from bottom to top. After mixture of resin and hardener was added into the mold, full insertion of fiber sensors was achieved in each specimen. After curation process of 48 hours at room temperature, the specimens were machined using CNC (Computer numerical control) machine in a star shape in which each leg represented the direction and placement of the fiber sensor, Figure 3a. The sample consisted of 5 mm of thickness and each leg of the star shape was 25 mm in width and approximately 200 mm in length, Figure 3b. Furthermore, the geometrical illustration of the star sample explained the location and direction of the fiber sensors in each lag and within the plies (through thickness), Figure 3d.

B. Experimental Procedure

The GF of Nylon/Ag fiber was tested experimentally as described in [63], Figure 4. The star specimen was placed between the rollers in the INSTRON-50 machine in such a manner that sensor A was along the roller axis and data acquisition system was attached to the electrode wires connected to the Nylon/Ag fiber sensors, Figure 5. It was vital to ensure that the sample was positioned properly among the rollers and the electrical connections were isolated from any metallic part of the machine to avoid any external influence on the electrical response of the fiber sensors. Then, the test was performed at low strain rate i.e. 2 mm/min up to 2 kN to avoid any permanent deformation and each test was performed for 10 cycles. The mechanical response of the specimen with the electrical profile of all four fiber sensors was obtained.

III. Results and Discussion

A. Electromechanical response and GF calculation of the Nylon/Ag fiber sensor

The results of Nylon/Ag fiber sensor showed that the resistance was gradually changing with the strain deformation which indicated good correlation between its electromechanical behavior, Figure 6a. GF showed high strain sensitivity of the fiber sensor and was calculated by calculating the change in the resistance during the strain deformation of the sensor as shown in eq. 1.

$$G.F \times \varepsilon = \Delta \frac{R}{R} \tag{1}$$

The GF of Nylon/Ag fiber sensor was found to be in between 21-25 with in the elastic limit [63], Figure 6b.

B. Deformation mechanism and mechanical characterization of composite star specimen

It was important to comprehend the flexural deformation of the composite sample to comprehend the signal of the Nylon/Ag fiber sensor. Star specimens were placed in the machine as simply supported beam with one leg of the specimen placed on the bottom rollers and flexural deflection and force was applied by the third roller at the center of the span length of the respective leg of the star sample, Figure 7a. Moreover, in each test sample was placed in the machine in such a way that sensor A was along the roller axis and the leg of the star sample with sensor C was between the three rollers i.e. along the span length. When the star samples were applied with the flexural deflection, the sample strained inside the span length and this deformation resulted in compression strain at the top surface (shown by green) because of the compressive forces applied by the roller whereas, this deformation caused tensile strain near the bottom surface because of the elongation (shown by red arrows), Figure 7b. Then these compressive and tensile deformations progressed through each ply from top and bottom surface and could result in macro damage such as fiber fracture, matrix cracking and/or interlaminar shear failure.

Three flexural tests were performed successfully. Sample 1 & 2 were placed in the machine in such a manner that sensor A was in the bottom position along the roller axis (case I) and the leg with sensor C was between the rollers. However, sample 3 was placed in the machine in such a manner that sensor A was in the top position, sensor D was in the bottom position (case II) while keeping the leg with sensor C between the rollers, Figure 8. This step was performed to test the sensitivity of the fiber sensor and its ability to detect and identify type of deformation with in the plies of composite under flexural deformation and results showed that it had no effect on the mechanical performance of the specimens with good repeatability in results, Figure 9. Moreover, experimental mechanical properties consisting of flexural strength, strain, and modulus were calculated using eq. (2)-(4)

$$\sigma_f = \frac{3FL}{2bd^2} \quad (2)$$

$$\varepsilon_f = \frac{6Dd}{L^2} \quad (3)$$

$$E_f = \frac{L^3 m}{4bd^3} \quad (4)$$

Where, σ_f is flexural stress, ε_f is flexural strain, E_f is flexural modulus of elasticity, *F* is the load at a given point on the load deflection curve, *L* is span length, *b* is width of specimen, *d* is thickness, *D* is deflection, and *m* is the gradient of the initial straight-line portion of the load deflection curve.

Moreover, the mechanical behavior of all the three star-samples was similar to each other regardless of the placement of the specimen. This further confirmed that the placement of fiber sensors at different positions [65] and directions did not influence the mechanical behavior and integrity of the composite sample and its isotropic nature. Although, it should be kept in mind that the objective of this study was to examine the sensitivity and in-situ monitoring response of the Nylon/Ag fiber sensor incorporated into the composite specimens subjected to cyclic flexural loading

C. In-situ monitoring and identification of strain deformation by Nylon/Ag fiber sensor

The resistance of Nylon/Ag fiber sensor changed gradually in each case with the strain applied and demonstrated good signal response but, when samples were deforming each fiber sensor inside the sample demonstrated unique signal response because of their specific position regarding the roller axis and position through the thickness. Test 1 and test 2 were conducted by performed by positioning the specimens in such manner that sensor A along the roller axis and was on the bottom position regarding the thickness or loading axis while the specimen of test 3 was positioned in such manner that sensor A was along the roller axis but was on the top position regarding the thickness or loading axis. The position of the other sensors i.e. B, C, and D was changed accordingly (as discussed previously, see Figure 8) however, the leg of the star specimen with sensor C remained the loaded leg in all two cases.

Å Test 1 and Test 2 validated the repeatability in electrical response and in-situ monitoring behavior of the fiber sensor. All four fiber sensors showed changed in resistance and correlated perfectly during mechanical deformation of the composite specimen in both tests, Figure 10. Also, it was detected that all fiber sensors were showing decrease in resistance with an increase in strain and vice versa. The magnitude of change in resistance of sensor C was maximum in comparison with sensor A, B and D.

Å Test 3 was conducted and related with test 1 to understand the sensitivity of the fiber sensor regarding the loading axis and placement through the thickness of the specimen, Figure 11. Sensor C which was place within the loaded leg in both cases showed opposite behavior and demonstrated the maximum increase in resistance in test 3 while other three sensors again showed decrease in resistance however, change in magnitude of each signal was recorded, Figure 11.

In both cases all 4 sensors showed interesting behavior and it was necessary to compare and discuss in detail the response of each fiber sensor sequentially to understand the deformation behavior of the composite star specimen.

Å Sensor A: as described earlier, it was placed in 0° direction with respect to the roller axis in both cases however, in case I it was positioned on the bottom while in case II it was positioned on the top. It should be kept in mind that this leg of the star specimen was not supported by the rollers and was not under the direct flexural load whether it was case I or II. This leg of the star specimen was only under the localized effect of the central roller which was applying the load and displacement to the specimen. This localized effect resulted in the detection of compression stresses that could be generated in the surface beneath the central roller. In addition, the increase in magnitude of the signal justified the position of the sensor A with respect to the loading axis/through thickness i.e. in case I it was at the bottom position where minimum compression strain was generated while in Case II it was on the top position where effect of the compression strain is maximum, Figure 12a.

Å Sensor B: as described earlier, sensor B was placed in 45° direction with respect to the roller axis in both cases however, in case I it was positioned second from the bottom while in case II it was positioned second from the top surface i.e. between the plies 2 and 3. This leg of the star specimen was also not supported by the rollers and was not under the direct flexural load whether it was case I or II. It was also only under the localized effect of the central roller which was applying the load and displacement to the specimen. This localized effect resulted in the detection of compression stresses that could be generated in the surface beneath the central roller. However, the magnitude of change in resistance of sensor B in comparison with sensor A in case I was more because it was closer to the effect of central roller than sensor A, Figure 10. In addition, when position of the specimen was changed in case II, sensor B showed increase in the magnitude of the signal in comparison with the signal of the sensor B in case I because of more effect of applied compression load by the central roller, Figure 12b. But this increase in magnitude was less than the increase in magnitude of the signal of sensor A in case II because when position of the specimen was change sensor A was more in contact with the central roller than sensor B where the effect of compression strain was higher, Figure 11.

Å Sensor C: as described earlier, sensor C was placed in 90° direction with respect to the roller axis in both cases however, in case I it was positioned third from the bottom while in case II it was positioned third from the top surface i.e. between the plies 3 and 4. This leg of the star specimen was the only segment of the star specimen supported by the rollers and was under the direct flexural load whether it was case I or II. The whole leg experienced the bending effect during the experiment and showed most interesting behavior. This sensor did not only showed change in the magnitude of the signal but also showed different deformation detection. In case I, sensor C showed decrease in resistance with the increase in the applied strain and the magnitude of the signal was maximum in comparison with sensor A, B, and D, Figure 12. This maximum magnitude of the signal in case I of sensor C was not only because of the fact that it was closer to the effect of the applied compression load by the roller but also because of the reason that this whole leg of the star specimen was deforming, and the sensor detected the overall deformation in the leg instead of localized deformation. In addition, when position of the specimen was changed in case II, sensor C was the only sensor showed increase in resistance with the increase in the applied strain in addition to the maximum magnitude of the signal in comparison with the other fiber sensors. The increase in resistance confirmed the detection of tensile deformation near the bottom surface of the composite star specimen and justified the deformation mechanism of the specimen which is subjected to flexural loading, Figure 11. However, the magnitude of the signal of the sensor C during the detection of tensile deformation was less than the magnitude of the signal during the detection of compression strain because of its position through the thickness of the specimen, Figure 12c.

Å Sensor D: as described earlier, it was placed in -45° direction with respect to the roller axis in both cases however, in case I it was positioned on the top while in case II it was positioned on the bottom. It should be kept in mind that this leg of the star specimen was not supported by the rollers and was not under the direct flexural load whether it was case I or II. This leg of the star specimen was only under the localized effect of the central roller which resulted in the detection of compression stresses that could be generated in the surface beneath the central roller. In addition, the decrease in magnitude of the signal justified the position of the sensor D with respect to the loading axis/through thickness i.e. in case I it was at the top position where maximum compression strain was generated while in Case II it was on the bottom position where effect of the compression strain is minimum, Figure 12d. It was also observed sensor A in case I and sensor D showed similar behavior and vice versa because in case I and II sensor A and D interchanged their position from top to bottom with respect to the thickness, Figure 11.

IV. Conclusions

An experimental study was performed in this research to examine and understand the application of Nylon/Ag fiber sensor in in-situ monitoring and identification of strain deformation in composites under cyclic flexural deformation. At first, the GF of Nylon/Ag fiber sensor was calculated experimental and was found with the range of 21-25. Then, the fiber sensor was integrated with in the composite specimen at specific direction and position to demonstrate the strain detection behavior of the Nylon/Ag fiber sensor and identification of different types of deformation which occurred during flexural deflection. The experimental results showed good repeatability in the mechanical performance of the composite structures and response of the fiber sensor in monitoring of the deformation. Each fiber sensor showed individual response signal during the deformation of the composite specimen because of their specific position and direction. This distinct behavior of each fiber sensor confirmed the detection of different type of damage i.e. tensile or compression during the deflection and different intensity or magnitude of the signals quantified the amount of damage induced. Thus, each fiber sensor not only showed detection of different types of deformation but also indicated whether the deformation was overall or localized. The Nylon/Ag fiber sensor demonstrated good potential as a flexible reinforcement in composite materials for in-situ monitoring of strain because the applied strain was up to 1-2% for 10 cycles and the Nylon/Ag fiber showed perfect correlation of its signal with the applied strain in each cycle. This verified the stability and durability of this fiber sensor.

V. References

[1] M. Tarfaoui, M. Nachtane, and A. El Moumen. (2019.). Energy dissipation of stitched and unstitched woven composite materials during dynamic compression test, *Composites Part B: Engineering*, 167, 487ï 496.

[2] O. H. Hassoon, M. Tarfaoui, A. El Moumen, Y. Qureshi, H. Benyahia, and M. Nachtane. (2019.). Mechanical performance evaluation of sandwich panels exposed to slamming impacts: Comparison between experimental and SPH results, *Composites Structures,* 220, 776ï 783

[3] M. Nachtane, M. Tarfaoui, S. Sassi, A. El Moumen, and D. Saifaoui. (2019.). An investigation of hygrothermal aging effects on high strain rate behaviour of adhesively bonded composite joints, *Composites Part B: Engineering*, 172, 111ï 120.

[4] S. Sassi, M. Tarfaoui, M. Nachtane, and H. Ben Yahia. (2019.). Strain rate effects on the dynamic compressive response and the failure behavior of polyester matrix, *Composites Part B: Engineering*, 174, 107040, 2019.

[5] J. W. C. Pang and I. P. Bond. (2005.). A hollow fibre reinforced polymer composite encompassing self-healing and enhanced damage visibility, *Composites Science and Technology*, 65(11), 1791ï 1799

[6] C. Dry. (1996.). Procedures developed for self-repair of polymer matrix composite materials, *Composites Structures*, 35(3), 263ï 269

[7] C. Dry and W. McMillan. (1997.). A novel method to detect crack location and volume in opaque and semi-opaque brittle materials,ò *Smart Materials and Structures*, 6(1), 35ï 39.

[8] J.-B. Ihn and F.-K. Chang. (2008.). Pitch-catch active sensing methods in structural health monitoring for aircraft structures, *Structural Health Monitoring,* 7(1),5ï 9.

[9] A. Loayssa, (2011) ñOptical Fiber Sensors for Structural Health Monitoring,ò *New Developments in Sensing Technology for Structural Health Monitoring*, S. C. Mukhopadhyay, Ed. Berlin, Heidelberg: Springer Berlin Heidelberg, 335ï 358.

[10] B. Lin and V. Giurgiutiu. (2007.). Modeling and testing of PZT and PVDF piezoelectric wafer active sensors, *Smart Materials and Structures*, 15, 1085.

[11] A. C. Raghavan and C. Cesnik. (2007.). Review of Guided-Wave Structural Health Monitoring, *Shock and vibration digest*, 39, 91ï 114.

[12] V. Zilberstein *et al.* (2003.). MWM eddy-current arrays for crack initiation and growth monitoring, *International Journal of Fatigue*, 25(9ï 11), 1147ï 1155.

[13] J. P. Lynch, K. H. Law, A. S. Kiremidjian, T. W. Kenny, E. Carryer, and A. Partridge, ñThe Design of a Wireless Sensing Unit for Structural Health Monitoring,ò in *3rd Int. Workshop on Struc. Heal. Monit.*, 2001.

[14] F.-G. Yuan, *Structural Health Monitoring (SHM) in Aerospace Structures*. Oxford, UK: Elsevier, 2016.

[15] J. E. Michaels. (2008.). Detection, localization and characterization of damage in plates with an in situ array of spatially distributed ultrasonic sensors, *Smart Materials and Structures*, 17(3).

[16] X. P. Zhu, P. Rizzo, A. Marzani, and J. Bruck. (2010.). Ultrasonic guided waves for nondestructive evaluation/structural health monitoring of trusses, *Measurement Science and Technology,* 21(4).

[17] Y. Shen, J. Zhong, S. Cai, H. Ma, Z. Qu, Y. Guo, Y. Li. (2019.). Effect of Temperature and Water Absorption on Low-Velocity Impact Damage of Composites with Multi-Layer Structured Flax Fiber. *Materials* 2019, 12, 453.

[18] D. Derusova, V. Vavilov, S. Sfarra, F. Sarasini, V. Krasnoveikin, A. Chulkov, S. Pawarf. (2019.). Ultrasonic spectroscopic analysis of impact damage in composites by using laser vibrometry, Composite Structures, 211, 221ï 228.

[19] F. Azhari and N. Banthia (2012.). Cement-based sensors with carbon fibers and carbon nanotubes for piezoresistive sensing, *Cement and Concrete Composites*, 34(7), 866ï 873

[20] G. Georgousis *et al.* (2015.). Study of the reinforcing mechanism and strain sensing in a carbon black filled elastomer, *Composites Part B: Engineering*, 80, 20ï 26

[21] J. Hoheneder, I. Flores-Vivian, Z. Lin, P. Zilberman, and K. Sobolev. (2015.). The performance of stress-sensing smart fiber reinforced composites in moist and sodium chloride environments, *Composites Part B: Engineering*, 73, 89ï 95

[22] J. M. Park, S.-I. Lee, K.-W. Kim, and D.-J. Yoon. (2001.). Interfacial Aspects of Electrodeposited Conductive Fibers/Epoxy Composites using Electro-Micromechanical Technique and Nondestructive Evaluation, *Journal of Colloid and Interface Science*, 237, 80ï 90.

[23] J.-M. Park, S.-I. Lee, and K. L. DeVries. (2006.). Nondestructive sensing evaluation of surface modified single-carbon fiber reinforced epoxy composites by electrical resistivity measurement, *Composites Part B: Engineering*, 37(7), 612ï 626.

[24] A. Todoroki, K. Yamada, Y. Mizutani, Y. Suzuki, and R. Matsuzaki. (2015.). Impact damage detection of a carbon-fibre-reinforced-polymer plate employing self-sensing time-domain reflectometry, *Composite Structures*, 130, 74ï 179.

[25] J. M. Park, D.-J. Kwon, Z.-J. Wang, J.-J. Kim, K.-W. Jang, and K. L. Devries. (2014.). New method for interfacial evaluation of carbon fiber/thermosetting composites by wetting and electrical resistance measurements, *Journal of Adhesion Science and Technology,* 28.

[26] D.-J. Kwon, Z.-J. Wang, J.-Y. Choi, P.-S. Shin, K. L. Devries, and J. M. Park. (2015.). Interfacial evaluation of carbon fiber/epoxy composites using electrical resistance measurements at room and a cryogenic temperature, *Composites Part A: Applied Sciend and Manufacturing*, 72.

[27] Z.-J. Wang *et al.* (2013.). Mechanical and interfacial evaluation of CNT/polypropylene composites and monitoring of damage using electrical resistance measurements,ò *Composites Science and Technology*, 81, 69ï 75.

[28] S. A. Grammatikos and A. S. Paipetis. (2012.). On the electrical properties of multi scale reinforced composites for damage accumulation monitoring, *Composites Part B: Engineering*, 43(6), 2687ï 2696.

[29] J. CagáŘ, J. Pelant, M. Kyncl, M. Kadlec, and L. (2019.). Michalcová, Damage detection in carbon fiberï reinforced polymer composite via electrical resistance tomography with Gaussian anisotropic regularization, *Structural Health Monitoring,* 18(5ï 6), 1698ï 1710.

[30] T. M. Johnson, D. T. Fullwood, and G. Hansen. (2012.). Strain monitoring of carbon fiber composite via embedded nickel nano-particles, *Composites Part B: Engineering*, 43(3), 1155ï 1163.

[31] A. Al-Dahawi, O. Öztürk, F. Emami, G. Yǝldǝrǝm, and M. ķahmaran. (2016.). Effect of mixing methods on the electrical properties of cementitious composites incorporating different carbon-based materials, *Construction and Building Materials*, 104, 160ï 168.

[32] M.-J. Lim, H. K. Lee, I.-W. Nam, and H.-K. Kim. (2017.). Carbon nanotube/cement composites for crack monitoring of concrete structures, *Composites Structures*, 180, 741ï 750.

[33] B. Christian. (2000.). Next generation structural health monitoring and its integration into aircraft design, *International Journal of Systems Science*, 31(11), 1333ï 1349.

[34] V. K. Varadan and V. Varadan. (2000.). Microsensors, microelectromechanical systems (mems), and electronics for smart structures and systems. *Smart Materials and Structures*, 9(6), 953ï 972.

[35] N. Trifigny, F. M. Kelly, C. Cochrane, F. Boussu, V. Koncar, and D. Soulat. (2013.). PEDOT: PSS-based piezo-resistive sensors applied to reinforcement glass fibres for in situ measurement during the composite material weaving process, *Sensors*, 13(8), 10749ï 10764.

[36] O. Atalay and W. R. Kennon. (2014.). Knitted Strain Sensors: Impact of Design Parameters on Sensing Properties, *Sensors*.

[37] S. Seyedin, J. M. Razal, P. C. Innis, A. Jeiranikhameneh, S. Beirne, and G. G. Wallace. (2015.). Knitted strain sensor textiles of highly conductive all-polymeric fibers, *ACS Applied Materials & Interfaces*, 7(38), 21150ï 21158.

[38] I. Jerkovic, V. Koncar, and A. Grancaric. (2017.). New textile sensors for in situ structural health monitoring of textile reinforced thermoplastic composites based on the conductive poly(3,4-ethylenedioxythiophene)-poly(styrenesulfonate) polymer complex, *Sensors,* 17(10).

[39] H. Cheng *et al.* (2013.). Textile electrodes woven by carbon nanotubeï graphene hybrid fibers for flexible electrochemical capacitors, *Nanoscale*, 5(8), 3428.

[40] K. Kawano, R. Pacios, D. Poplavskyy, J. Nelson, D. D. C. Bradley, and J. R. Durrant. (2006.). Degradation of organic solar cells due to air exposure, *Solar Energy Materials and Solar Cells*, 90(20), 3520ï 3530.

[41] S. Nauman, I. Cristian, F. Boussu, and V. Koncar, *Smart Sensors for Industrial Applications. Part V Piezoresistive, Wireless, and Electrical Sensors*, USA, K. Iniewski, 2013.

[42] Z. Wan, J. Guo, and M. Jia. (2015.). Damage detection of three-dimensional braided composite materials using carbon nanotube thread, *Science and Engineering of Composite Materials*, 24(2), 213-220.

[43] S. Wang *et al. (2017.).* Smart wearable kevlar-based safeguarding electronic textile with excellent sensing performance, *Soft Matter*, 13(13), 2483ï 2491.

[44] S. Nag-Chowdhury, H. Bellégou, I. Pillin, M. Castro, P. Longrais, and J. F. Feller. (2018.). Crossed investigation of damage in composites with embedded quantum resistive strain sensors (sQRS), acoustic emission (AE) and digital image correlation (DIC), *Composites Science and Technology*, 160, 79ï 85.

[45] Z. Chen, X. Liu, S. Wang, X. Zhang, and H. Luo. (2018.). A bioinspired multilayer assembled microcrack architecture nanocomposite for highly sensitive strain sensing, *Composites Science and Technology*, 164, 51ï 58.

[46] N. Hu, Y. Karube, M. Arai, T. Watanabe, C. Yan, and Y. Li. (2010.). Investigation on sensitivity of polymer/carbon nanotube composite strain sensor, *Carbon* , 48, 680ï 687.

[47] Alamusi, N. Hu, H. Fukunaga, S. Atobe, Y. Liu, and J. Li., Piezoresistive strain sensors made from carbon nanotubes based polymer nanocomposites, *Sensors*, 11, 10691ï 10723.

[48] T. C. Theodosiou and D. A. Saravanos. (2010.). Numerical investigation of mechanisms affecting the piezoresistive properties of CNT-doped polymers using multi-scale models, *Composites Science and Technology*, 70, 1312ï 1320.

[49] G. Wang *et al.* (2018.). Structure dependent properties of carbon nanomaterials enabled fiber sensors for in situ monitoring of composites, *Composites Structures*, 195, 36ï 44.

[50] G. Cai, M. Yang, Z. Xu, J. Liu, B. Tang, and X. Wang. (2017.). Flexible and wearable strain sensing fabrics, *Chemical Engineering Journal*, 325, 396ï 403.

[51] H. Yang *et al.* (2018.). Highly sensitive and stretchable graphene-silicone rubber composites for strain sensing, *Composites Science and Technology*, 167, 371ï 378.

[52] A. S. Barnard. (2012.). Modelling of the reactivity and stability of carbon nanotubes under environmentally relevant conditions, *Physical Chemistry*

Chemical Physics, 14(9).
[53] A. R. Murray *et al.* (2009.). Oxidative stress and inflammatory response in dermal toxicity of single-walled carbon nanotubes, *Toxicology.*, 257(3), 61ï 171.
[54] T. Kinkeldei, C. Denier, C. Zysset, N. Muenzenrieder, and G. Troester. (2013.). 2D Thin Film Temperature Sensors Fabricated onto 3D Nylon Yarn Surface for Smart Textile Applications, *Research Journal of Textile and Apparel information*, 17(2), 16ï 20, 2013.
[55] J. Xie, H. Long, and M. Miao. (2016.). High sensitivity knitted fabric strain sensors, *Smart Materials and Structures*, 25(10).
[56] D. Ryu, K. J. Loh, R. Ireland, M. Karimzada, F. Yaghmaie, and A. M. Gusman. (2001.). In situ reduction of gold nanoparticles in PDMS matrices and applications for large strain sensing. *Smart Structures and Systems,* 8(5), 471ï 486.
[57] R. X. Wang, X. M. Tao, Y. Wang, G. F. Wang, and S. M. Shang. (2010.). Microstructures and electrical conductance of silver nanocrystalline thin films on flexible polymer substrates.,ò *Surface and Coatings Technology*, 204(8), 1206ï 1210.
[58] K.-S. Kim *et al.* (2018.). Revisiting the thickness reduction approach for near-foldable capacitive touch sensors based on a single layer of Ag nanowire-polymer composite structure, *Composites Science and Technology*, 165, 58ï 65.
[59] N. Perkas, G. Amirian, S. Dubinsky, S. Gazit, and A. Gedanken. (2007.). Ultrasound-assisted coating of nylon 6,6 with silv er nanoparticles and its antibacterial activity, *Journal of Applied Polymer Science*, 104(3).
[60] O. Atalay, A. Tuncay, M. D. Husain, and W. R. Kennon (2016.). Comparative study of the weft-knitted strain sensors, *Journal of Industrial Textiles*, 46(5), 1212ï 1240.
[61] Y. Atwa, N. Maheshwari, and I. A. Goldthorpe. (2015.). Silver nanowire coated threads for electrically conductive textiles, *Journal of Materials Chemistry C*, 3(16), 3908ï 3912.
[62] Y. Qureshi, M. Tarfaoui, K. K. Lafdi, and K. Lafdi, (2019). ñNanotechnology and Development of Strain Sensor for Damage Detection,ò *Advances in Structural Health Monitoring*, InTech Open.
[63] Y. Qureshi, M. Tarfaoui, K. K. Lafdi, and K. Lafdi. (2019.). Real-time strain monitoring performance of flexible Nylon/Ag conductive fiber, *Sensors and Actuators A Physical*, 295, 612ï 622.
[64] Y. Qureshi, M. Tarfaoui, K. K. Lafdi, and K. Lafdi. (2019.). Real-time strain monitoring and damage detection of composites in different directions of the applied load using a microscale flexible Nylon/Ag strain sensor, *Structural Health Monitoring*.
[65] Y. Qureshi, M. Tarfaoui, K. K. Lafdi, and K. Lafdi. (2019.). Development of microscale flexible nylon/Ag strain sensor wire for real-time monitoring and damage detection in composite structures subjected to three-point bend test, *Composites Science and technology*, 181, 107693.

Yumna Qureshi is currently doing her Ph.D. in Mechanical Engineering at ENSTA Bretagne, Brest, France. Her research activities focus on study the electromechanical behavior of nanocomposites under quasi-static and dynamic loading. Moreover, she has expertise in numerical modeling, finite element analysis, modeling of damage criteria and behavior (specially in nano composites).

Mostapha Tarfaoui main expertise is focused on the composite and nanocomposites materials behaviour including the static and dynamic responses. His research activities articulate around the development of experimental, theoretical and numerical approaches for a better description of the elastic behaviour of damaged composite/nanocomposite material.

Khalil K. Lafdi is a high school student. Since 2016, Khalil has been involved in different research subjects, including the development of strain sensors using nanotechnology. He gained engineering experience through an internship at the University of Dayton.

Khalid Lafdi is a carbon specialist with expertise in the fields of carbon processing, physical properties and structural characterizations at all scale levels. At this time, He has more than 220 articles and chapters published and 4 patents with three major licensed technologies in nano-manufacturing in fall 2005
.

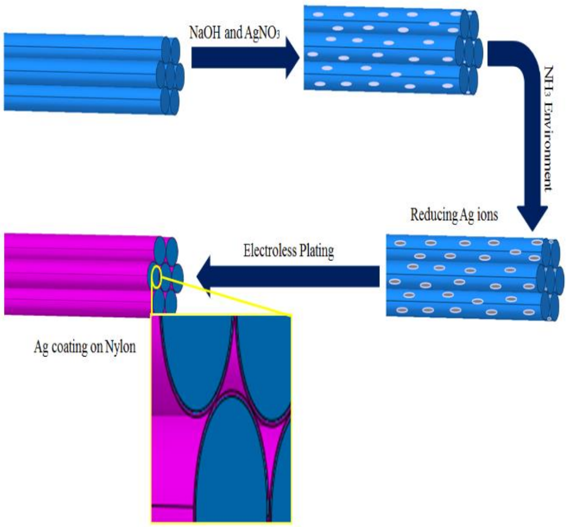

Fig. 1. Fabrication procedure of Nylon/Ag fiber sensor [63]

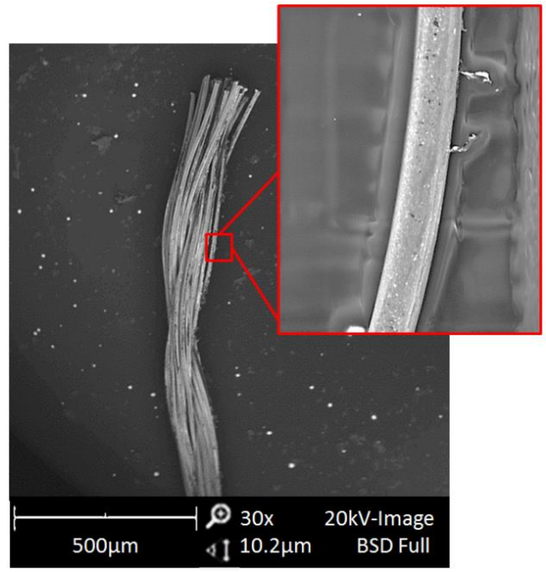

Fig. 2. SEM of Nylon/Ag fiber sensor after fabrication [64]

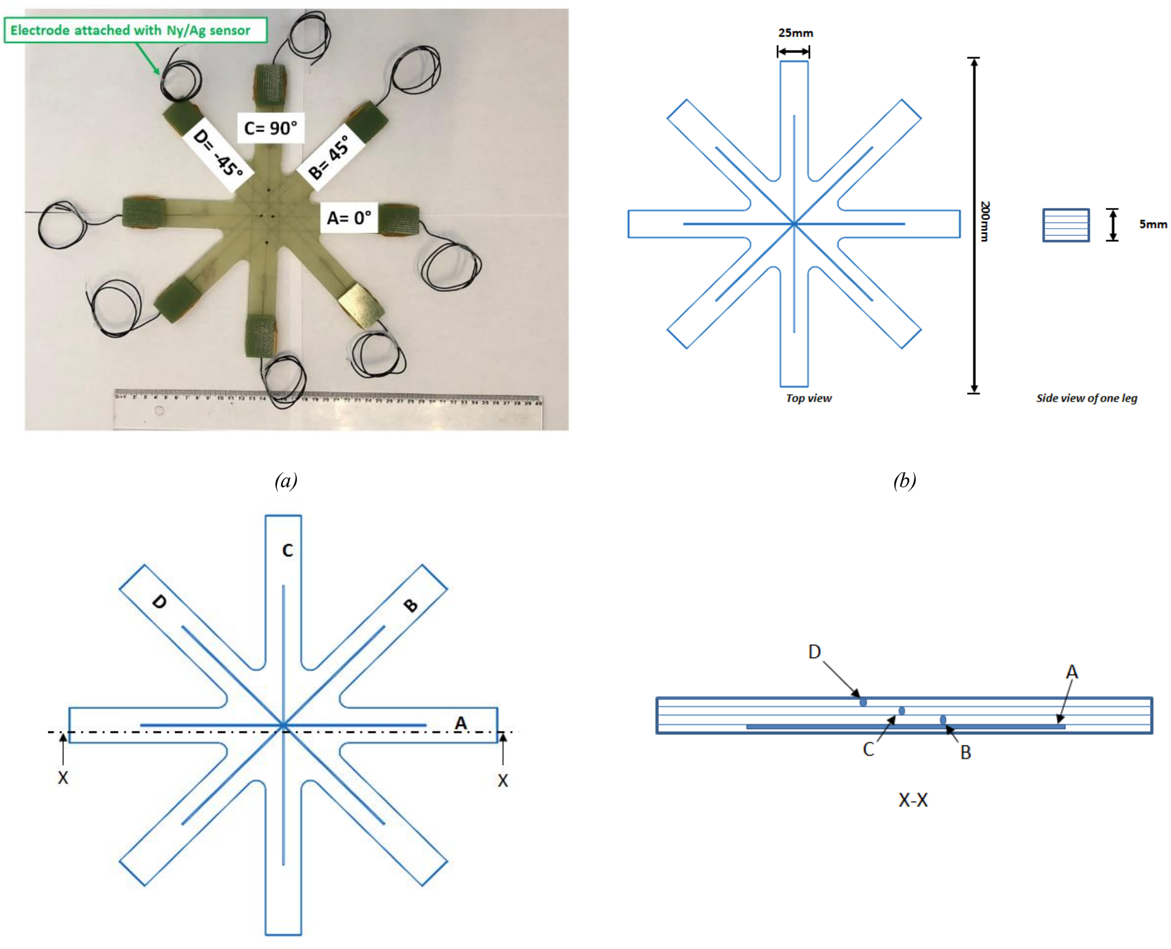

Fig. 3. (a) Composite sample turned transparent after the fabrication and embedded Nylon/Ag fiber sensors were visible in each leg. (b) Geometric parameters of the star samples. (c)-(d) Geometrical illustration of the placement of each Nylon/Ag fiber sensor in individual leg and through thickness (section view) correspondingly.

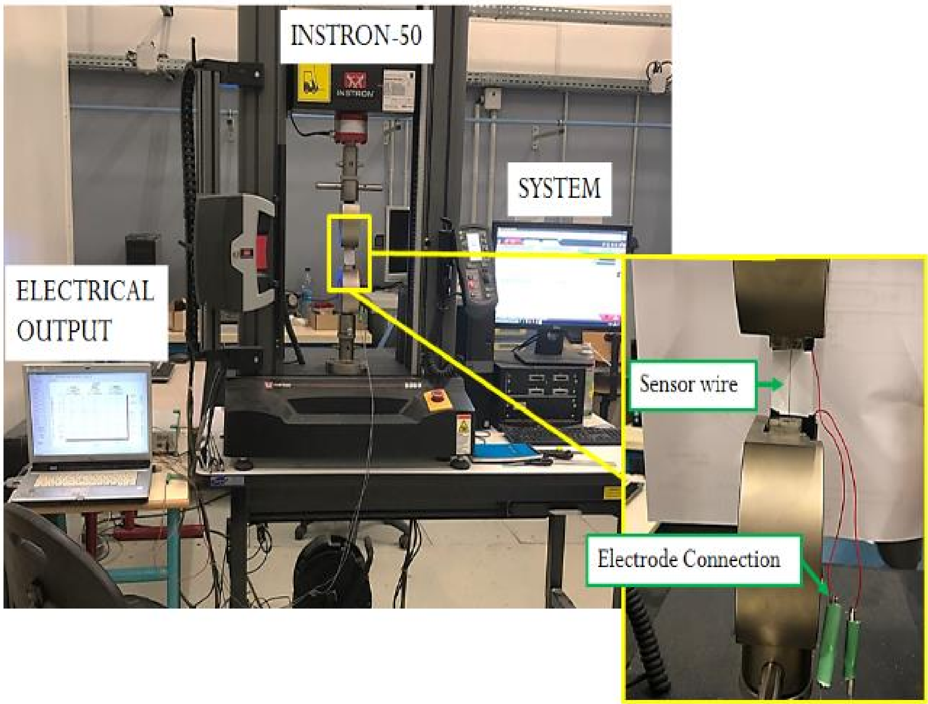

Fig. 4. Setup to examine the electromechanical response of the fiber sensor experimentally [63].

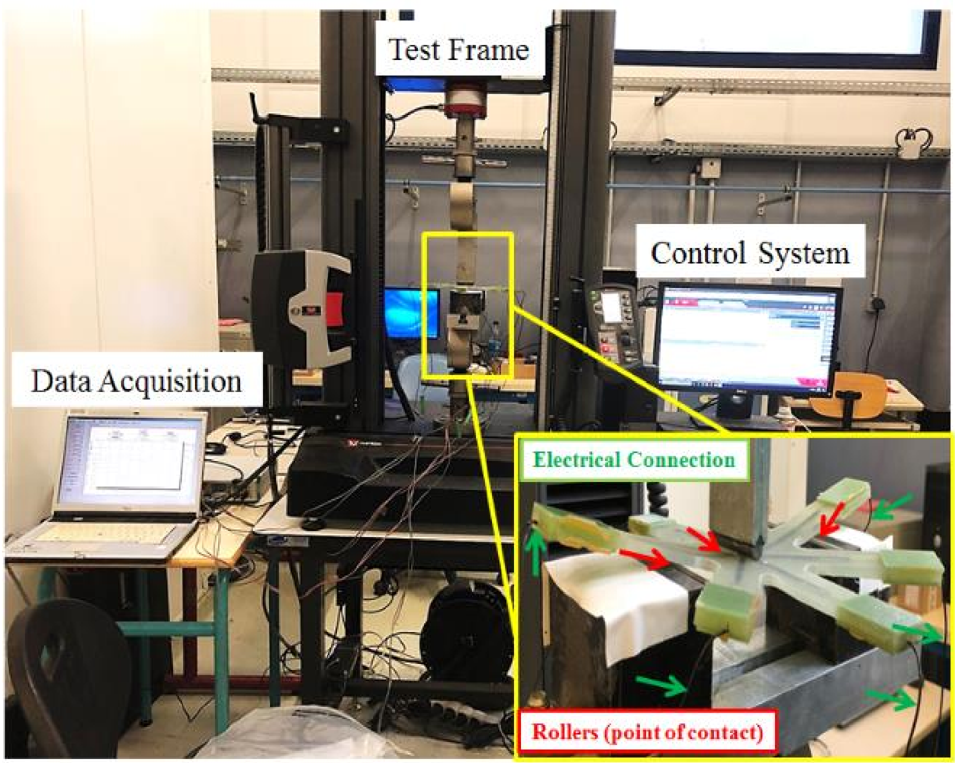

Fig. 5. Setup to examine the in-situ monitoring performance of the Nylon/Ag fiber sensor when integrated with in the composite sample during three-point bend test.

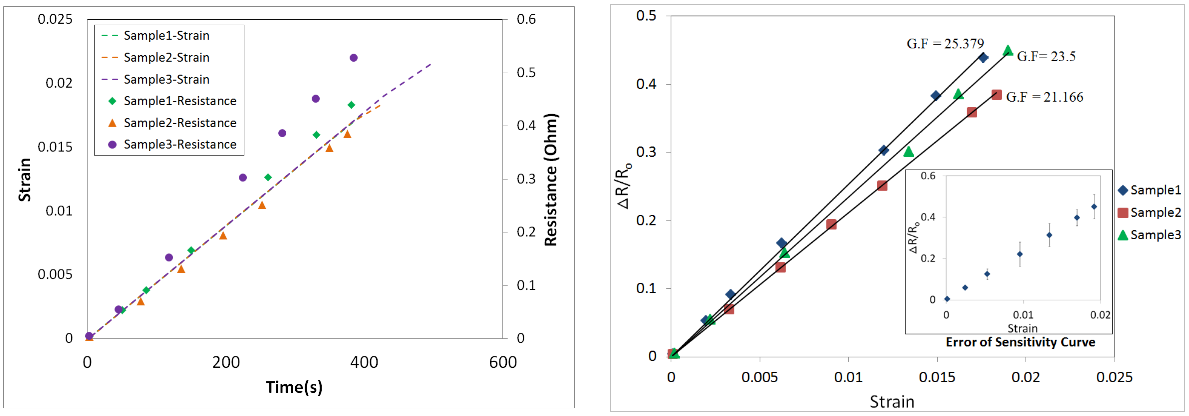

(a) *(b)*

Fig. 6. GF calculation of the Nylon/Ag fiber sensor. (a) shows that all three fiber sensor samples showed good electromechanical response. (b) shows the GF of all three samples with repeatability in results. Error of sensitivity curve was also plotted in this figure of all three samples [63].

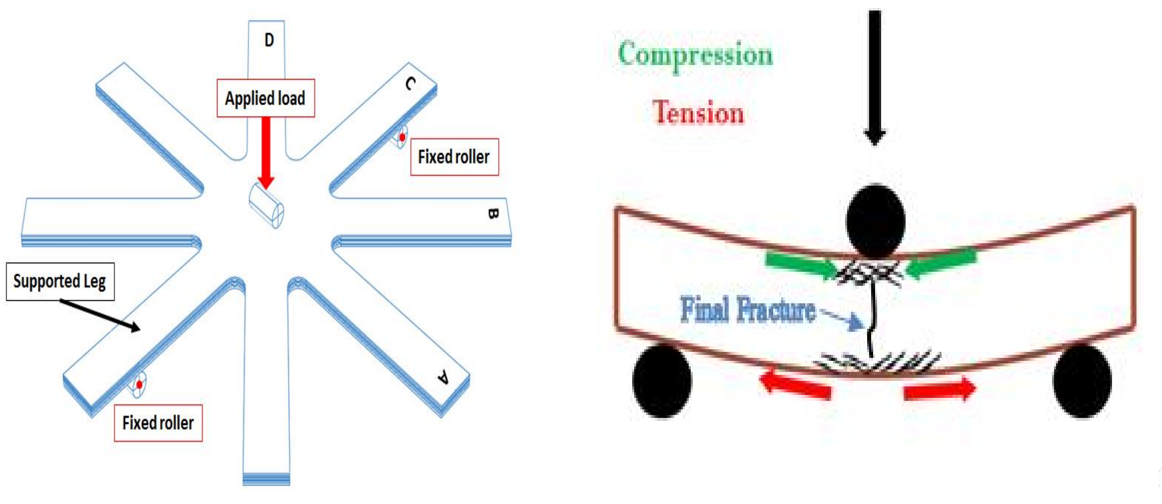

(a) Placement specimen in the machine *(b) Deformation behavior of the specimen*

Fig. 7. Deformation behavior of star specimen during three-point bend test.

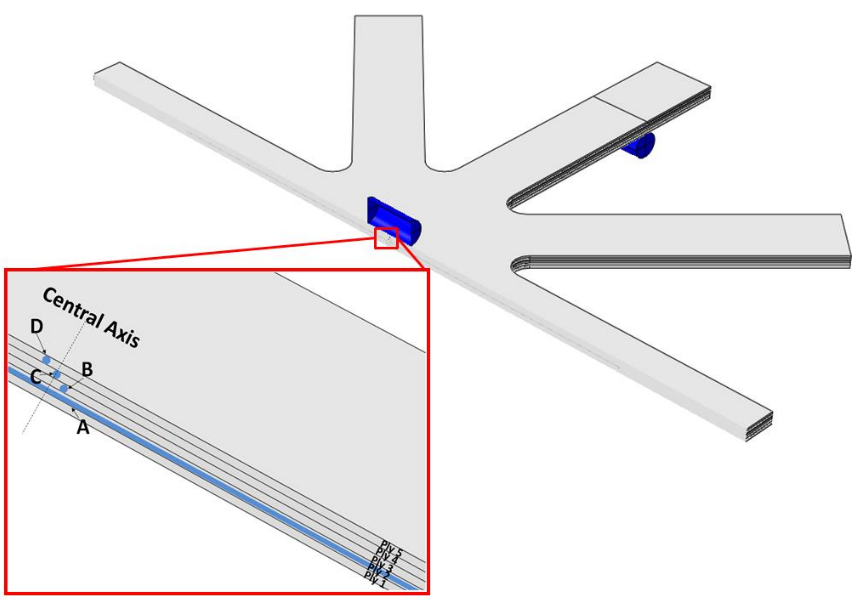

(a) Case I

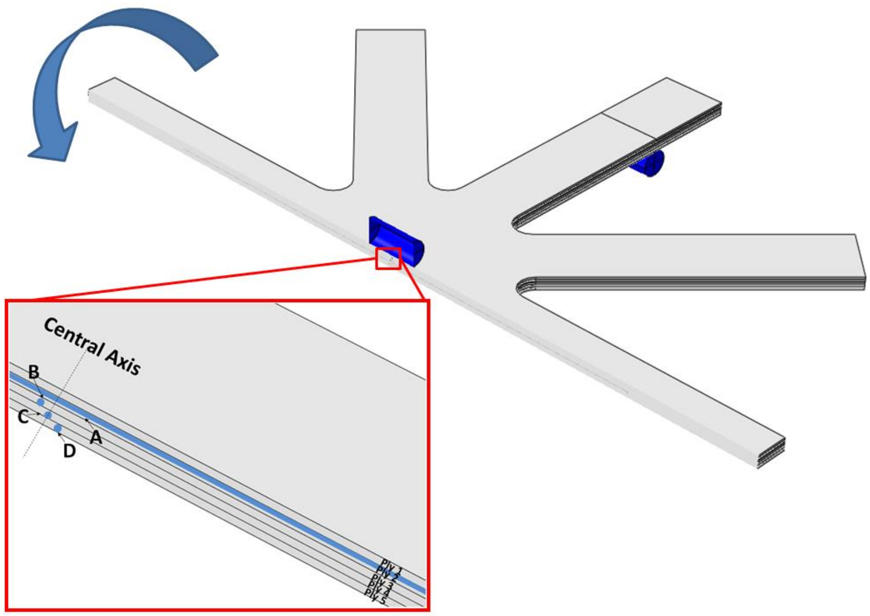

(b)Case II

Fig. 8. Position of the composite star samples between the three rollers for flexural bending: (a) Sample placement in test 1 and 2 when sensor A is at the bottom surface and sensor D is on the top while sensor C is in the loaded leg, (b) Sample placement in test 3 when sensor A is on the top and sensor D is in the bottom layer while sensor C is in the loaded leg.

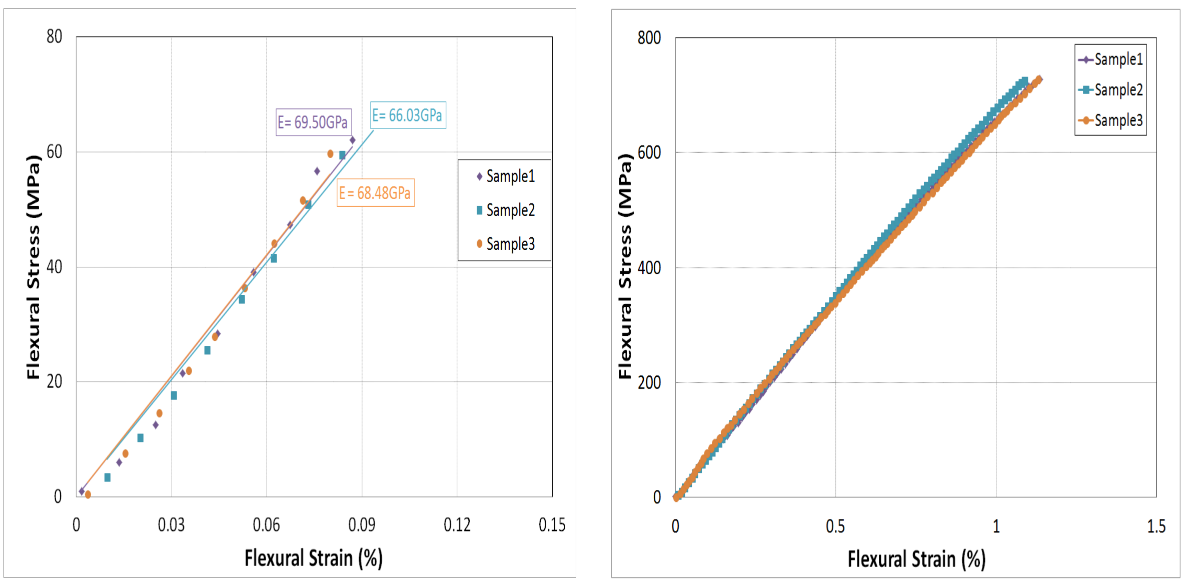

(a) *(b)*

Fig. 9. Mechanical behavior of all three star-samples. (a) Elastic modulus (b) Overall flexural stress-strain behavior

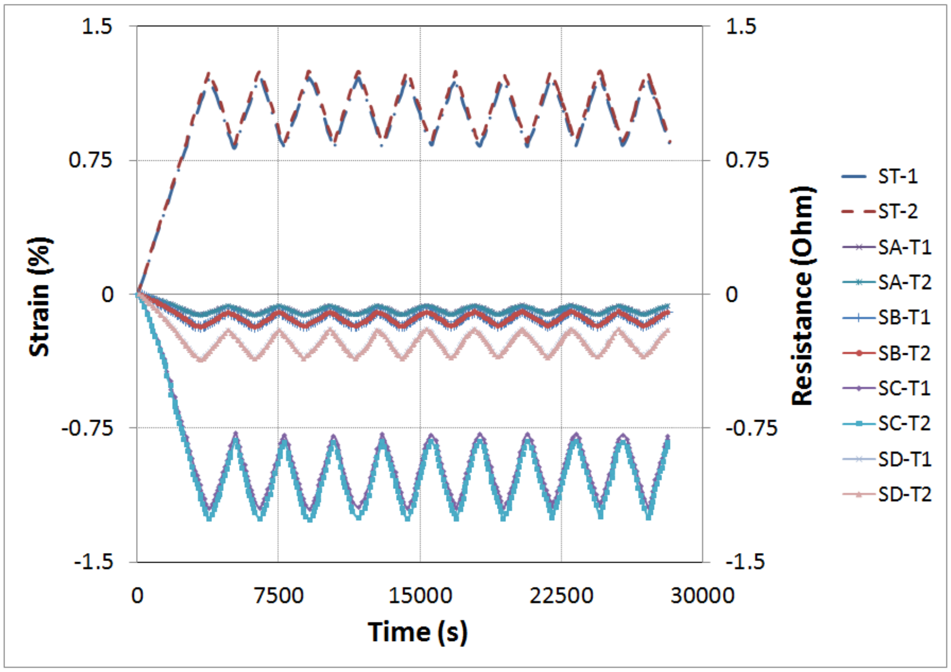

Fig. 10. In-situ flexural strain monitoring in composite star sample by Nylon/Ag fiber sensor and validation of electrical response of each fiber sensor.

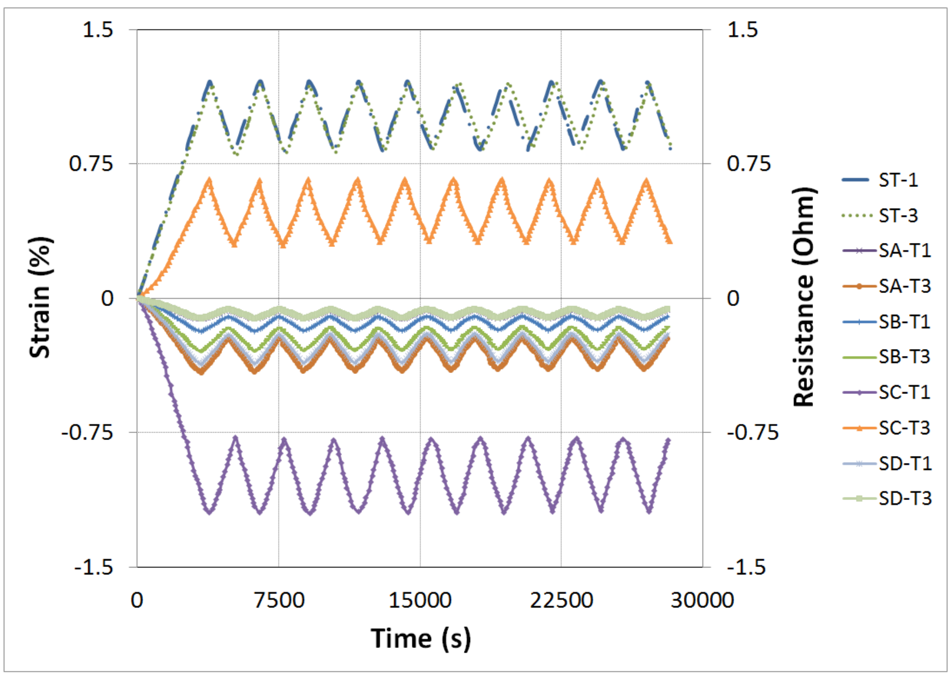

Fig. 11. In-situ flexural strain monitoring by Nylon/Ag fiber sensor and study of strain sensitivity of each fiber sensor with respect to its position. In test-1, sensor A was on the bottom position with respect to the loading axis, while in test-2 the specimen was rotated with respect to the roller axis and placed in such a manner that sensor A was on the top position with respect to the loading axis.

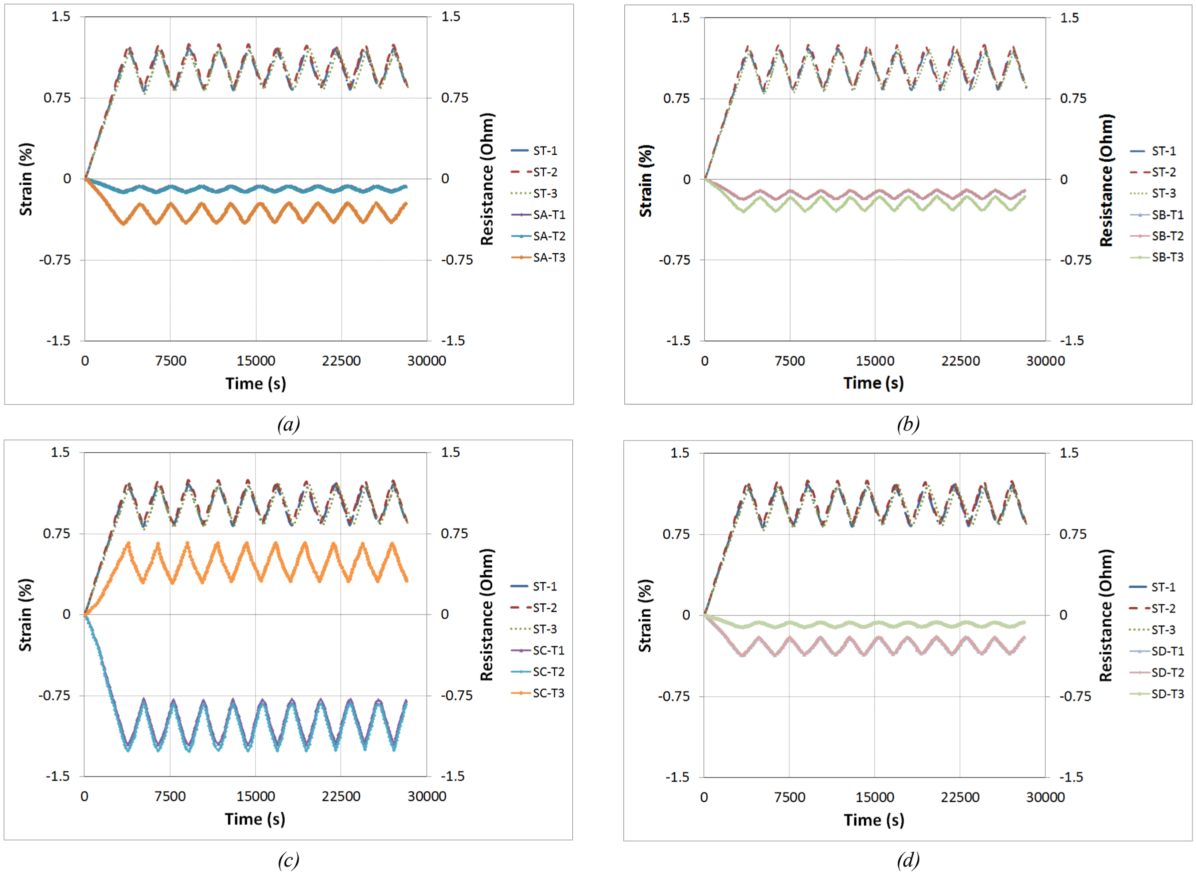

Fig. 12. In-situ monitoring and strain identification by Ny/Ag fiber sensor in each direction with respect to the roller axis and position with respect to the loading axis or through thickness